Superconductor Science and Technology

Additive manufacturing materials for structural optimisation and cooling enhancement of superconducting motors in cryo-electric aircraft

To cite this article before publication: Grant Lumsden *et al* 2023 *Supercond. Sci. Technol.* in press https://doi.org/10.1088/1361-6668/acf1d4

IOP Publishing Superconductor Science and Technology
Supercond. Sci. Technol. **XX** (XXXX) XXXXXX https://doi.org/XXXX/XXXX

Additive manufacturing materials for structural optimisation and cooling enhancement of superconducting motors in cryo-electric aircraft

Grant Lumsden[1], Bart Ludbrook[1], Nic Rogers Rehn[1], Fernando Solis Fernandez[1], Mike Davies[1], Vadim Chamritski[2], Sarat Signamneni [3], Rod Badcock[1]

[1] Robinson Research Institute, Victoria University of Wellington, Wellington, New Zealand
[2] HTS-110, Lower Hutt, New Zealand
[3] Department of Mechanical Engineering, Auckland University of Technology, Auckland, New Zealand

E-mail: grant.lumsden@vuw.ac.nz

Received xxxxxx
Accepted for publication xxxxxx
Published xxxxxx

Abstract

Superconducting electric motors offer the potential for low weight and high power in applications such as electric aircraft and high speed marine transport. Combined with renewably-sourced cryogenic fuels and advanced fuel cells they offer a path to zero-carbon mass transport. The proposed architectures of these extreme machines, operating at temperatures around 20K to 50K and employing very high alternating magnetic fields, require materials for the stator that are not electrically conducting and at the same time have good cryogenic structural performance.

Additively manufactured (AM) materials can play a key role in these designs, and a collaboration between the Robinson Research Institute and Auckland University of Technology is studying the performance of a range of composite polymers in superconducting machine applications. There are significant challenges to be met, including understanding the effect of the build process on material properties at low temperatures, and also the effect of formulation changes on thermal properties.

Additively manufactured metals can be employed in the rotor components, where the magnetic field fluctuations are very small for our synchronous designs. In this usage case, we can achieve dramatic reductions in the weight of the rotor assembly by minimising the number of joints and facilitating the design of multi-functional components in our helium cooled, vacuum cryostat architecture.

Novel design solutions have been developed for several key components in our prototype machines and these are discussed, along with cryogenic testing results for selected additively manufactured polymers and composites.

Keywords: Superconducting motors, Additive materials, Cryogenic design, Motor design, Material properties

1. Introduction

Superconducting motors and generators are key components in the roadmap for zero-carbon aviation [1], due to their ability to generate higher magnetic fields in a lighter and more compact package. However, this presents a number of design challenges due to the cryogenic temperatures, and rotating magnetic fields employed [2]. The Advanced Energy Technology Platform (AETP) is a multi-year programme [3] which aims to provide technology pathways that support electrification of mass transit, with a focus on demonstrating superconducting machine prototypes at progressively higher TRL levels.

Whilst a 20MW machine is the ultimate requirement for single-aisle electric aircraft thrusters [4], a 3MW device holds strong interest as both a generator and motor in a range of hybrid aircraft architectures that are envisaged [5,6]. Demonstrating such a device is the ultimate goal of the AETP programme and the team has developed the target specification summarized in Table 1 below [7]. The DC bus voltage is selected as 1,500 V with a 4 pole rotor, resulting in an electrical frequency of 150 Hz. An operating temperature of 40K is chosen for the field coils on the rotor to suit REBCO conductors operating at high current density, and the 3 MW motor will employ superconducting stator coils built with MgB_2 wire [8] operating at 20K which matches the current focus on liquid hydrogen (LH2) as a promising cryogenic fuel for aircraft applications [9].

Table 1. Design specifications for prototypes

Parameter	3 MW Motor Specs.	100kW Motor Specs.
Nominal rating, kW	3000	100
No. of Phases	3	3
DC bus voltage, V	1500	1500
Number of poles	4	4
Rated rotational speed, RPM	4500	4500
Rated frequency, Hz	150	150
Rotor field coil temp., K	40	40
Stator operating temp., K	20	300
Target specific power, kW/kg	>25	>5

To reduce risk, and aid in technology demonstration and component development, a subscale 100 kW motor will be built initially. The rotor for this 100 kW motor has broadly similar specifications as the 3 MW rotor, however it uses a stator built with copper conductor coils cooled to around room temperature with a suitable liquid.

In order to maximise the benefits from the use of superconductors and to minimise weight, an iron-free (or 'air-cored') design has been chosen [10]. Without an iron structure to shape the magnetic fields around the stator, the rotating fields have a greater propensity to generate eddy currents in any nearby conductors, such as aluminium or titanium structural components. Glass reinforced polymer composites become the logical material solution in many instances for the stator. Additionally, as we have chosen a synchronous motor architecture, the rotating components *can* be electrically conducting but the challenges around cooling these components are significant.

In order to create robust and lightweight designs for both the static and rotating structures, additive manufacturing (AM) methods are being used to maximise material utilization and enable multi-functional geometries for say, simultaneous cooling and structural performance. As part of our work, both metal and polymer additive materials and techniques are being evaluated for both cryogenic and 'room temperature' thermal environments.

Although some composites have been regularly used in cryogenic applications [11], there is a general lack of information on the cryogenic properties of AM polymeric materials. One thread in our current research addresses this gap through experimental evaluation of a growing set of materials, processed by selective laser sintering and fused deposition modelling [12]. The team at Auckland University of Technology is also building cryogenic materials data on high strength AM metals [13] which will be critical for rotor components.

As well as building confidence in our motor design and analysis capabilities, our ultimate goal is to use these insights to guide development of new material options with enhanced cryogenic properties.

2. Electrical design of 100kW and 3MW motors

The target architecture for these prototype motors incorporates rotor-mounted superconducting field coils and armature coils on the stator. This enables us to minimize weight and volume of the motor, whilst also allowing us to address the AC-loss thermal loads on the stator side rather than the rotor side.

Electrically powered thrusters are envisaged to be efficient across a wider operating speed range than gas turbines, so a synchronous design supplied via a DC bus and inverter has been selected.

Some relevant motor electrical parameters are shown in Table 2. For aircraft applications, one of the main benefits of a superconducting design for a high powered motor is the ability to trade off voltage for current. For motors with copper windings, lower currents mean lower resistive losses and the design trade-off tends to favour higher voltages, which are undesirable in an aircraft application. With a super-conducting design, a relatively low phase voltage can be specified and the

resulting high phase currents can be achieved with low losses and low weight.

Table 2. Electrical parameters for 100kW and 3MW prototype motors

Motor Parameter	3 MW Specs	100 kW Specs
Apparent Power, KVA	3280	130
Motor Real Power, KW	3220	127
Phase voltage, Vrms	602	357
Phase Current, A	1820	121
Field excitation current, A	3770	2900
Field Amp-turns per pole (kAt)	108	70

In Table 1, we note that the target specific power for the 3MW motor-generator is greater than 25kW/kg, however there are numerous technologies that need to be developed before this value can be approached [1]. Electrical, mechanical and cryogenic improvements are needed, and for this reason, the 100kW motor will have a much lower specific output, and will be used to raise the Technology Readiness Level (TRL) on key engineering systems that can then be implemented on the 3MW motor at more optimised weight values.

2. Cryogenic concepts for 100kW and 3MW motors

The 100 kW prototype motor is being built as a testbed for the superconducting rotor, and as such will use a conventional room temperature stator. The 3MW motor, in contrast, will feature a fully superconducting stator.

In both cases the rotors will carry the field coils, which are contactlessly energised using a DC 'flux pump' current [7]. The operating DC current in the coils will be in the order of 3000 to 3800A, but the rotor will produce relatively small electrical losses, estimated in the range of 4-5W for the 100kW motor, and 8-10W for the 3MW motor, and these are simply due to small resistances in the joints in the superconducting cables. The target operating temperature for the conductors is approximately 40K and the main thermal losses from both rotors will be conduction in the structural components. The rotor structure in both cases is necessarily a vacuum cryostat, to insulate the conductors and minimise the cooling load. A breakdown of the estimated heat losses for the 100kW machine is shown below in Table 3. We will confirm the overall thermal load during testing, and expect that this will allow us to use a commercially available stirling cryocooler for the rotor cooling.

For the 100kW motor, the stator will be operating in the range of 320-340K and the air gap between the rotor and stator will be air at ambient conditions. For the 3MW motor, in contrast, the stator will operate at around 20K, and therefore require its own cryostat. The simplest approach for this motor is to build a separate cryostat for the stator, and retain the ambient temperature air gap between the rotor and stator cryostats. This does significantly increase the clearance between the armature and field windings, however, which reduces the maximum field in the gap and reduces the maximum torque that can be developed. We refer to this as the 'warm gap' configuration.

Table 3. Estimated thermal loads for 100kW rotor

Heat source	Value
Conduction through driveshafts, W	15
Radiation losses, W	4
Coil electrical losses, W	5

An alternative approach for the 3MW motor would be to evacuate the 'air gap' and bring the rotor coils much closer to the stator, allowing them to be radiatively cooled by the 20K stator assembly. Design and analysis of a solution with this 'cold gap' architecture is currently in progress. As the success of the cold gap architecture is dependent on an integrated rotor and stator design, we will work with the warm gap approach initially as it affords greater development flexibility.

A variety of configurations have been used in the past to cryogenically cool the rotors of superconducting motors and generators [14][15]. To achieve the desired temperatures on our two 'warm gap' rotors, we have proposed using a dedicated cryocooler. This is an established approach [16] [17] and we are evaluating two implementations that will be described in the following sections.

3. Rotor for 100kW motor

The first rotor being built for the 100 kW motor will utilise a convection cooling scheme, where gaseous helium is circulated through a heat exchanger attached to the cold head of the rotor cryocooler. The helium circuit is pumped using a novel cooling circuit arrangement that allows the cryocooler to remain in the stationary frame, and required only a single helium seal. The vacuum cryostat is statically sealed and the helium seal is the only dynamic seal. The helium flows through longitudinal cooling passages in a "cooling core" that the superconducting field coils are bolted to.

Additive manufacturing techniques and materials have been found to offer substantial benefits in the design of the helium circuit. Figure la shows the initial design of the rotor structure, with the CORC field windings shown for reference. A 316L stainless steel was selected as the 'baseline' material for this, the primary structural component of the rotor, due to its well-understood thermal and mechanical performance under cryogenic conditions. The initial design used numerous machined components that were bolted together to form the cooling core.

Figure 1b shows a cutaway of the cooling core redesigned using an AM stainless steel 316L material, formed via a selective laser sintering (SLS) process. Details for room temperature properties are given in Table 4 below.

Table 4. AM 316L Stainless Steel specifications (room temperature)

Parameter	Value
Tensile Strength, MPa	590-700
Tensile Modulus, GPa	185
Elongation, %	25-55
Layer height, mm	0.07

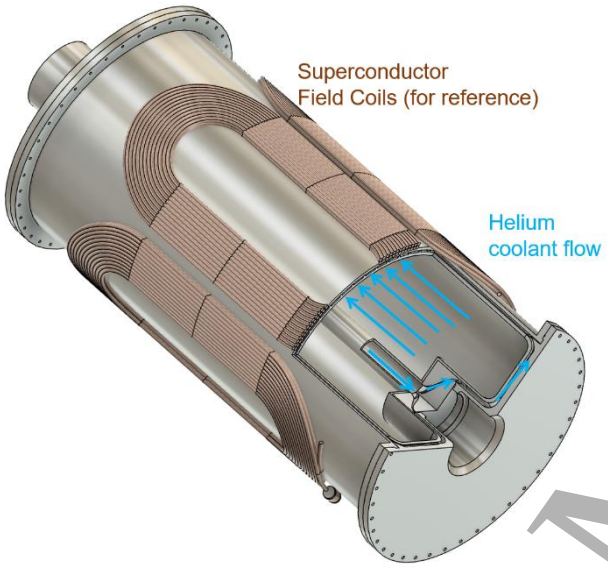

(a)

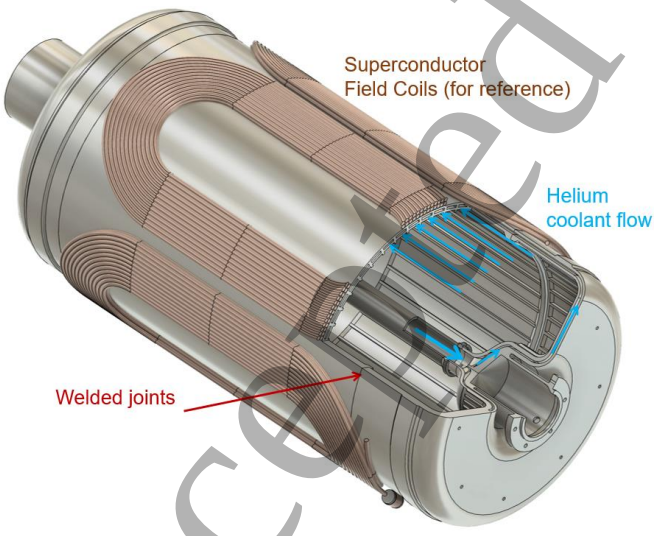

(b)

Figure 1: (a) Original rotor cooling structure with bolted joints (b) Rotor cooling structure using A.M techniques

Comparing the designs in Figure la and 1b, we find that the AM part weighs 13 kg and can be made by welding four printed parts together and then post-machining to achieve the necessary tolerances for mating parts. The conventionally designed part was made of 8 discrete machined components and 80 bolts. Due to the cryogenic vacuum nature of the environment, indium metal seals were required. The overall weight of the conventional part was 20 kg. The AM approach therefore represents a 35% saving in mass for this sub-system and these benefits are indicative of savings in other areas of the motor as well.

Figure 2: Sectioned components of AM stainless steel superconducting rotor cooling core

Test sections of the cooling core structure are shown in Figure 2. The claimed consolidation is 100% and we initially manufactured test pieces to evaluate vacuum and helium tightness.

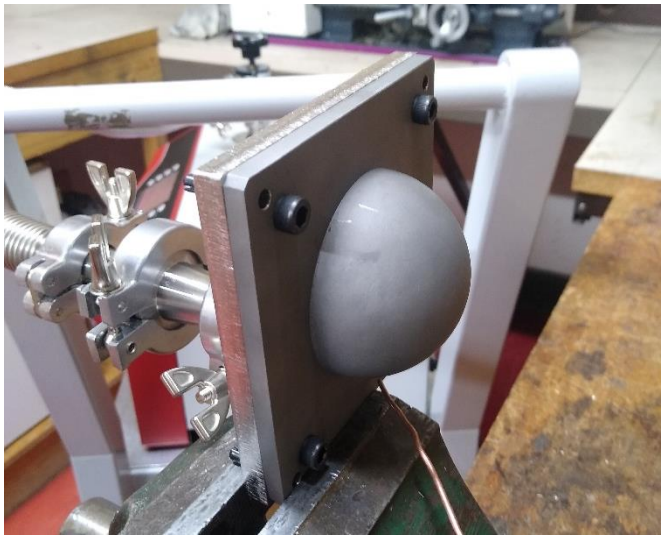

Figure 3: AM 2mm wall thickness SS316L dome test piece in helium-vacuum test rig.

A domed test part was manufactured with a 2mm wall thickness that is representative of the components we are designing. This was fitted to our helium leak test rig as shown

in Figure 3. The part achieved a vacuum of 5.4e-7 mbar and no pressure change was observed when exposed to helium on the high pressure side.

A second cylindrical test part was printed with a 1mm wall thickness and this was welded to a machined component to evaluate the weld integrity of the AM material in a practical application. This part also achieved 5.4e-7mbar of vacuum with the welded area under representative loading. This gives us good confidence that the printed 316L material can provide us with a robust and vacuum-capable basis for our designs.

Another feature of the rotor that benefits from our additive manufacturing research is the winding structure for the superconducting field coils. These will be wound using CORC cables [18] and need to be wound into the saddle shape in order to maximise the field developed, in absence of iron for flux routing. The saddle shape is achieved by winding into a former, and the coils must then be bonded in order to retain their shape. As shown in Figure 4, the solution that we have developed is to wind the coils onto a shaped bobbin that is held in the winding fixture. The coils are then bonded in place to the bobbin/former and the whole assembly can then be removed from the fixture and attached to the cooling core.

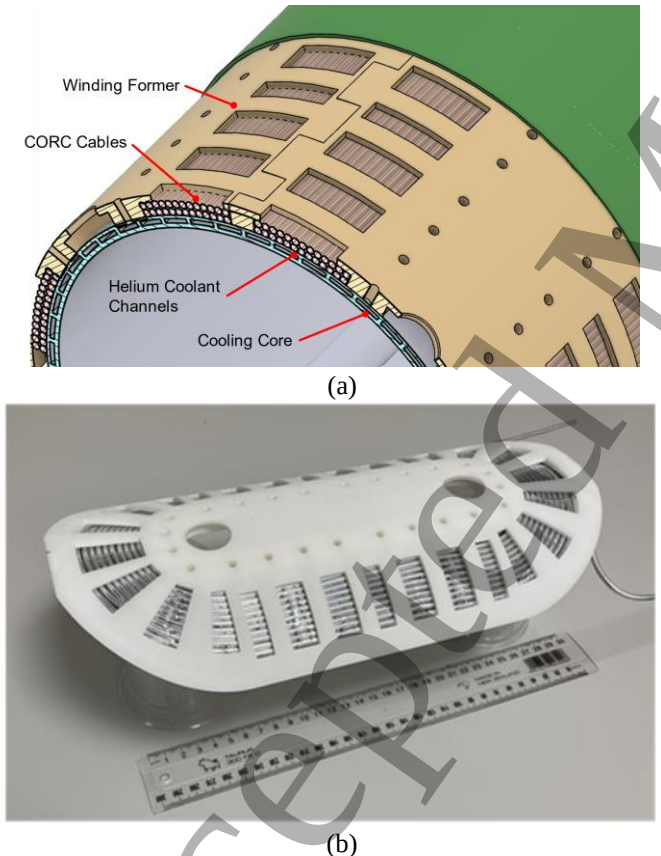

Figure 4: (a) Rotor coil design with integrated former for convection cooled rotor (b) test winding on AM integrated former.

Both the integrated former and the winding fixtures are manufactured using AM techniques. We have previously reported on the materials characterisation work that has been carried out [12] and based on these results we have selected a commercial printed SLS nylon with glass fill to provide the structural integrity and cryogenic performance that the former needs.

The integrated former is a structural component when assembled to the cooling core as it locates the coils relative to the rotor and each other, as well as reacting the torque generated by the coil itself and Lorentz forces on the winding, in conjunction with an external G10 sleeve.

4. Rotor for 3MW motor

For the 3 MW motor, we intend to simplify the rotor cooling further by eliminating the helium coolant and directly cooling the rotor coils conductively from the cryocooler cold head. Figure 5 shows a section view of the 3 MW motor with the layout of the main components. For this design, our team has proposed a rotating cryocooler [19], where the stirling cooler components are located co-axially with the rotor, and move with them. The coils that excite the linear drive to power the motor are stationary, however. This motor is currently under development and when available will give us the ability to significantly simplify the design.

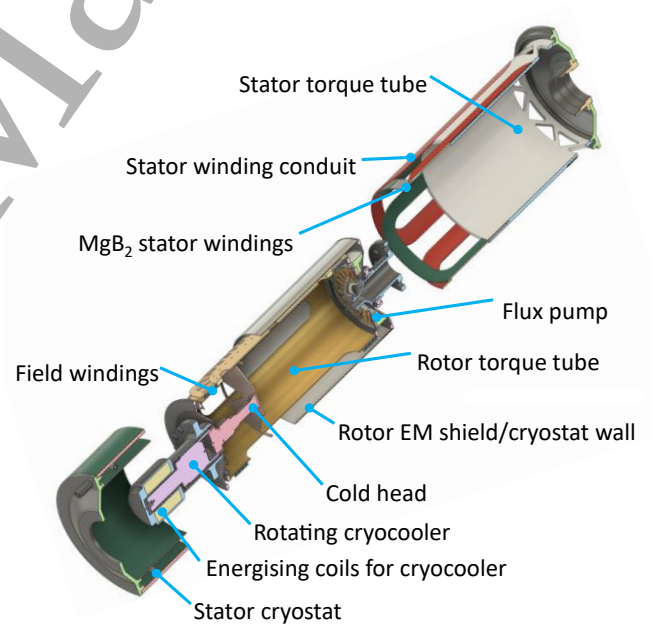

Figure 5: Exploded section layout of 3MW motor with conduction cooled rotor.

Additive materials have also been used in the preliminary design and analysis work for both the cryocooler components and the structural elements of the rotor itself. With a simpler cryostat arrangement, compared to the conduction – cooled

motor, we have been able to design AM parts that provide structural support for torque transfer whilst also being compliant to thermal contraction and presenting a minimal path for heat losses.

5. Stator for 100 kW motor

The stators for both motors can similarly benefit from AM manufacture. As the stator for the 100 kW motor is an air-cored design, the stator components are susceptible to the high frequency rotating field and can be inductively heated. Composite designs can be used to minimise these effects [20]. In addition, the stator of the 100 kW motor is a copper winding that must be positively cooled in order to achieve the current density required.

Figure 6 shows an exploded view of the fully-composite stator for the 100 kW motor and as with the rotors, an integrated winding bobbin/former is employed to wind the coils and these assemblies are then integrated into the stator structure. The stator conductors are cooled by immersion in a non-conducting fluid coolant, and the AM approach has enabled us to fine tune the coolant flow, using features to route and restrict coolant passages as needed. Figure 7a shows output from the CFD analysis, with flow lines and velocities calculated for the stator winding pack. The aim is to achieve a minimum flow velocity in all areas adjacent to the copper windings in order to avoid nucleate boiling that can occur when flow stagnates.

Figure 7b shows a simplified representation of the flowlines shown in Figure 7a, and it illustrates how the outer-layer winding former (in white) has been designed with features to route the cooling flow across both the outer layer winding and also down to the inner layer winding. The consistently turquoise-coloured flow tubes in Figure 7a that run under the outer layer former (see Figure 6a for component names) indicate an area of consistent flow velocity across the active lengths of the inner layer windings. The coolant flows in this area have thus been balanced and homogenised to enhance the overall cooling performance of the stator.

In these components we use an AM polymer (PA11, discussed further in Section 7) for the former components, and filament wound G10 tubes to provide the main structural support.

6. Stator for 3 MW motor

The stator for the 3MW motor presents additional challenges, and we are only at the early stages of design analysis. This motor will utilise superconducting windings in the stator, and these will need to be cooled to 20K using gaseous helium under pressure. The conventional approach to this is "conductor in conduit" (CIC) [21] where the conductor is run inside an insulated tube and helium flows through the tube to effect cooling.

Our initial concept for a wound coil is to run several conductors in a single conduit as shown in Figure 8. Due to the extremely high currents achievable, only a small number of turns will be required (see Table 2).

The conductors are likely to be multi-filament MgB_2 cables. These have a complex manufacturing process and, in general, are made into circuits using the "form and react" method [22], whereby the "green" wire must be shaped into a coil and then reacted in a furnace at around 700°C to create the actual superconductor.

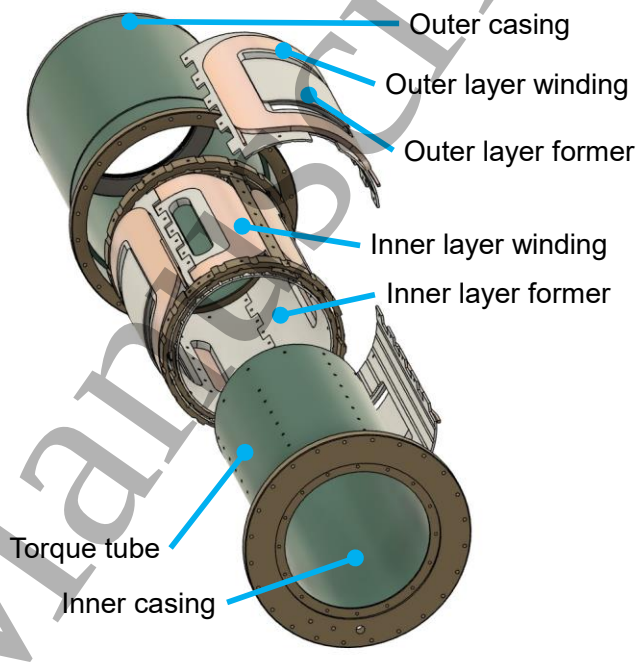

(a)

(b)

Figure 6: (a) Exploded view of 100 kW air-core copper stator. (b) AM inner-layer former and winding jig with G10 filament wound torque tube.

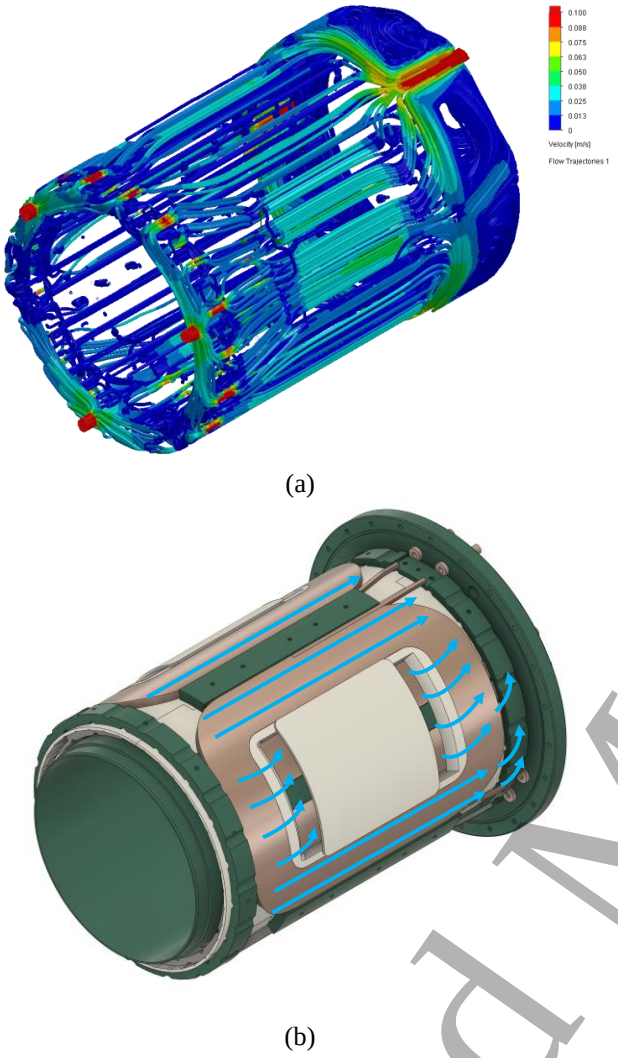

Figure 7: (a) CFD analysis streamlines and velocities in saddle-wound 100kW iron-free stator. (b) Simplified representation illustrating how flow is directed across the windings using AM features in the winding formers.

As we want the stator to be non- conducting, this approach presents significant challenges. Recent work on both zirconia [23] and alumina [24] AM processes gives us a number of interesting design approaches for the CIC fabrication. Our current concept design involves creating an AM ceramic coil former that we can wind the MgB_2 onto, and then react the wire in the furnace. The ceramic provides excellent turn to turn electrical isolation as well as structural support. When fixed into a composite conduit, Helium can flow freely around the wires, providing the necessary cooling. The AC currents in the stator coils will generate substantially higher losses than the DC currents in the rotor [25] .

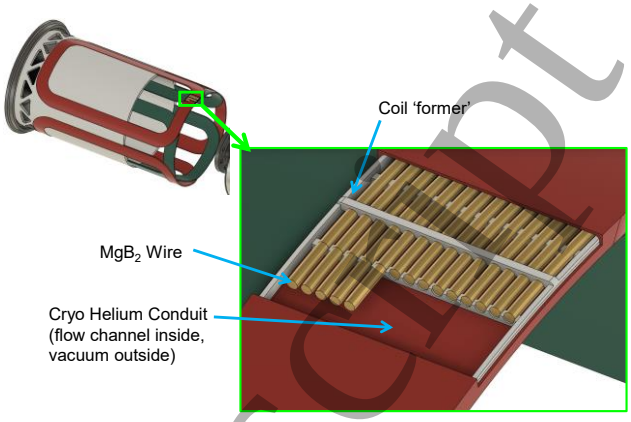

Figure 8: Cutaway view of MgB_2 conductor-in-conduit stator design concept.

Our present assumption is that helium for cooling the stator will, in turn, reject heat to a sink that is likely to be liquid hydrogen. The team at AUT have been working on this problem, designing compact heat exchangers to work between the hydrogen and helium fluids [26]. A number of novel configurations are being assessed that capitalise on the capabilities of AM metal processing.

7. Material properties characterisation

Aviation motor designs will rely heavily on AM materials in order to achieve the light weight, cooling performance and manufacturability needed for a robust aviation solution. Although AM materials are numerous and readily available from commercial printing agencies, there is a relatively small amount of information available about their properties under cryogenic conditions [27].

Our research group is working to build on that base of knowledge by testing both commercially available materials and developing new formulations. As previously noted, our team has measured the cryogenic properties of commercially available AM polymers [12] and AM metals [13]. A selection of the materials that have been tested to date are listed in Table 5. These represent a range of polyamide based engineering polymers that are available from commercial print agencies, and which are candidate materials for components in both the rotor and stator cryogenic structures. However, to design with these materials requires cryogenic characterisation.

Materials were evaluated using a Perkin Elmer DMA 8000, and a Tinius Olsen tensile tester. The DMA is used to measure material stiffness as a function of temperature and this unit can carry out evaluations over a temperature range from approximately 80K to room temperature. Strain-rate dependent properties can also be measured, but our current test

program is focused on low-frequency (1 Hz) measurements to provide data comparable to the static tensile tests.

Coupons were printed for both machines; an ASTM D638 dog-bone for tensile testing and a simple beam for the DMA, as shown in Figure 9(a). Samples were conditioned in a vacuum oven for >24hrs at 70ºC to achieve a consistent 'dry' condition. Tensile testing using the Tinius Olsen was carried out in general accordance with ASTM D638. The testing speed was 5mm/min, and specimens were stabilized at either 77K or 292K prior to testing. 77K tests were conducted with specimens immersed in liquid nitrogen at atmospheric pressure.

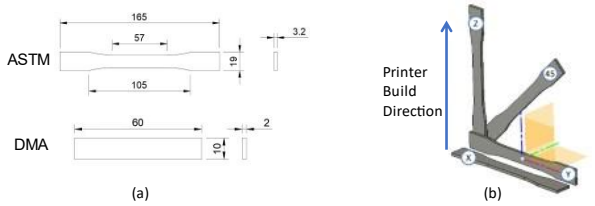

Figure 9. Test coupons: (a) dimensions in mm and (b) build orientation designation

The DMA modulus data from five tested materials in the 'X' orientation is shown in Figure 10. All materials show a clear transition around 130K as observed in other polymers [28], except the PA6-MF and Alumide which show an unexpected, almost linear response to temperature.

In this series of tests we also decided to investigate the influence of build orientation on the mechanical performance. In practice, most parts will have a range of orientations of load relative to build plane. Test coupons for the materials were therefore produced in a variety of orientations which we designated as shown in Figure 9(b).

Table 5. Materials tested

Item	Designation	Base polymer	Filler
1	PA12-GF40	Polyamide-12	Glass
2	PA6-MF	Polyamide-6	Mineral
3	PA12	Polyamide-12	None
4	PA11	Polyamide-11	None
5	Alumide	Polyamide-12	Aluminium powder

The effect of build direction on the PA24-GF40 material is shown in Figure 11, as an example, and we have demonstrated that this is important to consider in the design process if they are to be used for structural components [12].

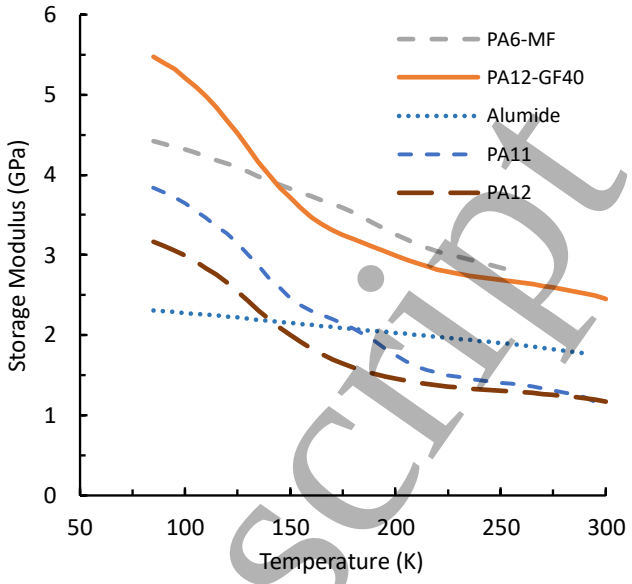

Figure 10: Test data for a selection of commercially available AM polymer materials. Effect of temperature on modulus.

This work on materials characterisation is an ongoing thread in our research workstream, and we anticipate building a library of materials characteristics over time in order to inform our prototyping work.

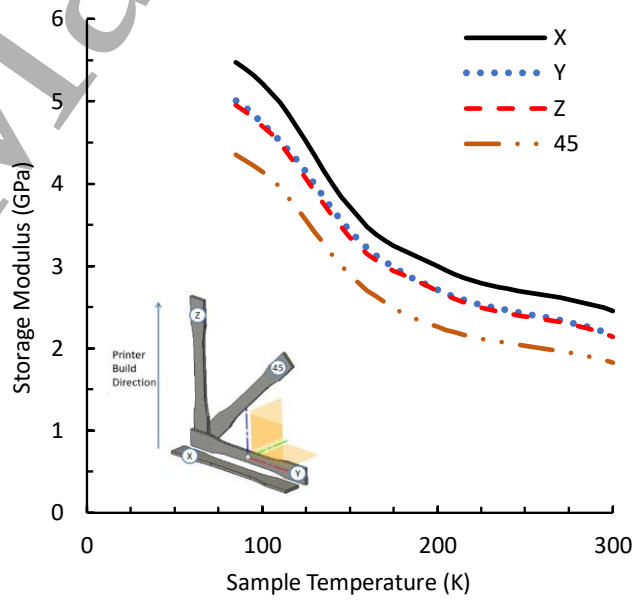

Figure 11: AM polymer (Polyamide12 with 40% glass powder fill) modulus as a function of temperature, illustrating the effect of build orientation.

8. Conclusions

Building an electric motor that is fully superconducting and can approach the power density required for aviation applications requires the solving of many significant

engineering challenges in the areas of cryogenic design, electromagnetic design and cooling system development.

As we work through these challenges in the build of our first two prototype motors, additive manufacture processes are providing significant opportunities for multi-functional design. Our designs are utilising AM polymers, metals and ceramics to this end.

We will continue to report on the subsequent improvements in performance, and also on the ongoing work to characterise AM materials at cryogenic conditions.

Acknowledgements

This work was supported by the Ministry of Business, Innovation and Employment, New Zealand, under the Advanced Energy Technology Platform program "High power electric motors for large scale transport", contract number RTVU2004

References

[1] K. S. Haran et al., "High power density superconducting rotating machines - Development status and technology roadmap," Supercond. Sci. Technol., vol. 30, no. 12, 2017, Art. no. 123002.

[2] C. D. Manolopoulos, M. F. Iacchetti, A. C. Smith, K. Berger, M. Husband, and P. Miller, "Stator Design and Performance of Superconducting Motors for Aerospace Electric Propulsion Systems," IEEE Trans. Appl. Supercond., vol. 28, no. 4, pp. 1–5, Jun. 2018, doi: 10.1109/TASC.2018.2814742.

[3] R. Badcock, H. Weijers, A. Caughley, et al., "High power density electric motors for large-scale transport," presented at the CEC/ICMC 2021, J3Or1A-03 [Invited], Jul. 2021.

[4] P. Kshirsagar, S. Dwari, J. M. Rheaume, R. Taylor, C. E. Lents, and P. Walsh, "Anatomy of a 20 MW Electrified Aircraft: Metrics and Technology Drivers," in AIAA Propulsion and Energy 2020 Forum, Aug. 2020. doi: 10.2514/6.2020-3581.

[5] J. Hoelzen et al., "Conceptual Design of Operation Strategies for Hybrid Electric Aircraft," Energies, vol. 11, no. 1, p. 217, Jan. 2018, doi: 10.3390/en11010217.

[6] P. Bertrand, T. Spierling, and C. E. Lents, "Parallel Hybrid Propulsion System for a Regional Turboprop: Conceptual Design and Benefits Analysis," in AIAA Propulsion and Energy 2019 Forum, Indianapolis, IN: American Institute of Aeronautics and Astronautics, Aug. 2019.

[7] S. S. Kalsi, J. G. Storey, J. M. Brooks, G. Lumsden, and R. A. Badcock, "Superconducting Synchronous Motor Development for Airplane Applications - Mechanical and Electrical Design of a Prototype 100 kW Motor," IEEE Trans. Appl. Supercond., vol. 33, no. 5, pp. 1–6, Aug. 2023,

[8] C. D. Manolopoulos, M. F. Iacchetti, A. C. Smith, K. Berger, M. Husband, and P. Miller, "Stator Design and Performance of Superconducting Motors for Aerospace Electric Propulsion Systems," IEEE Trans. Appl. Supercond., vol. 28, no. 4, pp. 1–5, Jun. 2018, doi: 10.1109/TASC.2018.2814742.

[9] J. K. Noland, C. M. Hartmann, and R. Mellerud, "Next-generation cryoelectric hydrogen-powered aviation: A disruptive superconducting propulsion system cooled by onboard cryogenic fuels," IEEE Ind. Electron. Mag., vol. 16, no. 4, pp. 6–15, Dec. 2022.

[10] S. Kalsi, "Influence of Magnetic Iron Teeth in Motors Employing Superconductors for Field Excitation and AC Stator Windings," IEEE Trans. Appl. Supercond., vol. 31, no. 4, pp. 1–7, Jun. 2021, doi: 10.1109/TASC.2021.3062485.

[11] A. F. Clark, R. P. Reed, and G. Hartwig, Eds., Nonmetallic Materials and Composites at Low Temperatures, Boston, MA: Springer US, 1979. DOI: 10.1007/978-1-4615-7522-1.

[12] G. Lumsden, S. Singamneni, B. Ludbrook, H. Weijers, and R. A. Badcock, "Additively Manufactured Polymer Composites for Superconducting Motor Coil Structures," IEEE Trans. Appl. Supercond., vol. 33, no. 5, pp. 1–5, Aug. 2023, doi: 10.1109/TASC.2023.3260762.

[13] O. Edwards et al., "Cryogenic characterisation of selective laser melted cobalt chromium," Materials Today: Proceedings, p. S2214785323024525, May 2023, doi: 10.1016/j.matpr.2023.04.526.

[14] J. J. Scheidler, "Preliminary Design of the Superconducting Rotor for NASA's 1.4 MW High-Efficiency Electric Machine," in 2018 Joint Propulsion Conference, Cincinnati, Ohio: American Institute of Aeronautics and Astronautics, Jul. 2018. doi: 10.2514/6.2018-4617

[15] F. Spaven, Y. Liu, R. Bucknall, T. Coombs, and M. Baghdadi, "Thermal design of superconducting cryogenic rotor: Solutions to conduction cooling challenges," Case Studies in Thermal Engineering, vol. 28, p. 101423, Dec. 2021, doi: 10.1016/j.csite.2021.101423.

[16] R. W. Dyson, P. Passe, K. P. Duffy, and R. Jansen, "High Efficiency Megawatt Motor Rotating Cryocooler Conceptual Design," in AIAA Propulsion and Energy 2019 Forum, Indianapolis, IN: American Institute of Aeronautics and Astronautics, Aug. 2019. doi: 10.2514/6.2019-4515.

[17] J. Xiao, T. Balachandran, A. J. Samarakoon, and K. S. Haran, "A Spoke-Supported Superconducting Rotor With Rotating Cryocooler," IEEE Trans. Magn., vol. 58, no. 8, pp. 1–5, Aug. 2022, doi: 10.1109/TMAG.2022.3150786.

[18] D. C. van der Laan, J. D. Weiss, and D. M. McRae, "Status of CORC ® cables and wires for use in high-field magnets and power systems a decade after their introduction," Superconductor Science and Technology, vol. 32, no. 3, p. 033001, Mar. 1, 2019, ISSN: 0953-2048, 1361-6668. DOI: 10.1088/1361-6668/aafc82.

[19] S. Jeong et al., "Holistic approach for cryogenic cooling system design of 3 MW electrical aircraft motors," in AIAA Propulsion and Energy 2021 Forum, Aug. 2021. doi: 10.2514/6.2021-3297.

[20] Y. Zhou, H. Xu, Q. Xiong, X.-J. Niu, and R.-G. Xie, "Design, Performance Analysis, and Testing of Composite Components for the Oil-Cooling Air-Core Stator of a High Temperature Superconducting Motor," IEEE Trans. Appl. Supercond., vol. 31, no. 8, pp. 1–5, Nov. 2021.

[21] L. Muzzi, G. De Marzi, A. Di Zenobio, and A. della Corte, "Cable-in-conduit conductors: lessons from the recent past for future developments with low and high temperature superconductors," Supercond. Sci. Technol., vol. 28, no. 5, p. 053001, May 2015, doi: 10.1088/0953-2048/28/5/053001.

[22] Z. Zhang, J. MacManus-Driscoll, H. Suo, and Q. Wang, "Review of synthesis of high volumetric density, low

gravimetric density MgB2 bulk for potential magnetic field applications," Superconductivity, vol. 3, p. 100015, Sep. 2022, doi: 10.1016/j.supcon.2022.100015.

[23] X. Zhang, X. Wu, and J. Shi, "Additive manufacturing of zirconia ceramics: a state-of-the-art review," Journal of Materials Research and Technology, vol. 9, no. 4, pp. 9029–9048, Jul. 2020, doi: 10.1016/j.jmrt.2020.05.131.

[24] S. Mamatha, P. Biswas, P. Ramavath, D. Das, and R. Johnson, "3D printing of complex shaped alumina parts," Ceramics International, vol. 44, no. 16, pp. 19278–19281, Nov. 2018, doi: 10.1016/j.ceramint.2018.07.153.

[25] S. S. Kalsi, R. Badcock, J. Storey, K. A. Hamilton, and Z. Jiang, "Motors Employing REBCO CORC and MgB 2 Superconductors for AC Stator Windings," IEEE Trans. Appl. Supercond., vol. 31, no. 9, pp. 1–7, Dec. 2021, doi: 10.1109/TASC.2021.3113574.

[26] O. Bonner-Hutton et al., "Analysis of gyroid heat exchangers for superconducting electric motors," Materials Today: Proceedings, p. S2214785323018527, Apr. 2023, doi: 10.1016/j.matpr.2023.03.780.

[27] K.-P. Weiss, N. Bagrets, C. Lange, W. Goldacker, and J. Wohlgemuth, "Thermal and mechanical properties of selected 3D printed thermoplastics in the cryogenic temperature regime," IOP Conf. Ser.: Mater. Sci. Eng., vol. 102, p. 012022, Dec. 2015, doi: 10.1088/1757-899X/102/1/012022.